

# Optical coupling of an active microdisk to a passive one: effect on the lasing thresholds of the whispering-gallery supermodes

Elena I. Smotrova\* and Alexander I. Nosich

Laboratory of Micro and Nano Optics, Institute of Radio-Physics and Electronics NASU, Kharkiv 61085, Ukraine

\*Corresponding author: elena.smotrova@gmail.com

Received April 16, 2013; revised May 13, 2013; accepted May 13, 2013;  
posted May 13, 2013 (Doc. ID 188898); published June 5, 2013

The lasing spectra and thresholds of a selectively pumped photonic molecule composed of two microdisks is investigated using effective index approximation and full-wave 2-D electromagnetic equations. The lasing eigenvalue problem formulation is used to find modal frequencies and threshold values of material gain. The influence of the optical coupling between active and passive microdisks on the lasing eigenvalues and directionalities of emission is studied. It is shown that for strong coupling the effect of making one of the resonators passive leads to the doubling of the threshold. © 2013 Optical Society of America

OCIS codes: (140.0140) Lasers and laser optics; (140.3560) Lasers, ring; (140.3945) Microcavities; (140.3410) Laser resonators.

<http://dx.doi.org/10.1364/OL.38.002059>

Optically coupled passive microcavities, also called photonic molecules (PMs), and their active counterparts, PM microcavity lasers, keep attracting the attention of both experimentalists and researchers engaged in their modeling and simulation [1–12]. The reason for this is a hope to achieve efficient power combining and overall improvement of performance needed in high-density photonic integrated circuits. The simplest configuration of this sort is a pair of identical microdisks. If pumped, they display the lasing on coupled optical modes (also called supermodes) of different classes of symmetry [3–6].

To extract lasing frequency spectra and thresholds, a specifically tailored lasing eigenvalue problem (LEP) was proposed earlier [4,13,14]. In [4], we studied the LEP for a PM formed by a pair of optically coupled *identical active* microdisks with uniform gain supporting the whispering-gallery (WG) modes. It was found that the threshold of lasing for each supermode might be lower than for a similar WG mode in a single microdisk. Later this study was extended to cyclic photonic-molecule lasers made of circular cavities [5], where an even larger threshold reduction was found.

In this Letter we present some results of the LEP analysis of a PM composed of *one active* and *another passive* microdisk of the same diameter  $a$  and refractive index  $\alpha$ , as shown in Fig. 1. Such a configuration can be obtained either if only one disk contains quantum wells or electrodes or is doped with erbium, or if optical pumping is done with a focused beam illuminating only one of two disks. Our goal is a study of the effect of optical coupling on the thresholds and directionalities of emission. Note that this analysis is completely out of reach for the conventional Q-factor study of a passive PM cavity.

Suppose that only the right-hand disk (No. 1) is active and has uniform bulk material gain,  $\gamma > 0$ , so that its complex refractive index is  $\nu_1 = \alpha - i\gamma$ , while  $\nu_2 = \alpha$ , and the host medium is air. Separation between the disks is denoted  $w$ , time variation is  $\exp(-i\omega t)$ , free-space wave-number is  $k = \omega/c = 2\pi/\lambda$ , and  $\lambda$  is the wavelength.

Assume that the dimensionality of the modeling has been already reduced from 3-D to 2-D using the

effective-refractive index approximation, as is usual for thin flat dielectric cavities. In 2-D, one can treat two polarization states separately with the aid of a function  $U$ , which is either  $E_z$ - or  $H_z$ - field component. The LEP statement implies (see [14]) that  $U$  must satisfy the Helmholtz equation with corresponding coefficients in each material domain. At the disk rims, tangential components continuity conditions are imposed. In addition, the condition of the local power finiteness is to be satisfied. Considering the LEP, we look for two real numbers,  $\kappa = ka$  and  $\gamma$ . The first of them is the normalized frequency, while the second is the threshold material gain needed to make  $k$  real. Thanks to the real-valued  $k$ , we stipulate that  $U$  obeys the usual 2-D Sommerfeld radiation condition at  $(x, y) \rightarrow \infty$  and thus does not diverge at infinity. Each eigenvalue depends on the separation  $w$  and refractive index  $\alpha$  in continuous manner on the plane  $(\kappa, \gamma)$ .

The geometry in Fig. 1 has one line of symmetry that is the  $x$  axis. Therefore all possible field functions split to two different independent classes of symmetry with respect to that axis. Taking into account local power finiteness, we expand the field function inside cavities in the local polar coordinates  $(\rho_{1,2}, \varphi_{1,2})$  as

$$U_{1,2}(\rho, \varphi) = \sum_{p=(0)1}^{\infty} A_p^{1,2} J_p(k\nu_{1,2}\rho_{1,2}) S_p(\varphi_{1,2}), \quad \rho_{1,2} < a, \quad (1)$$

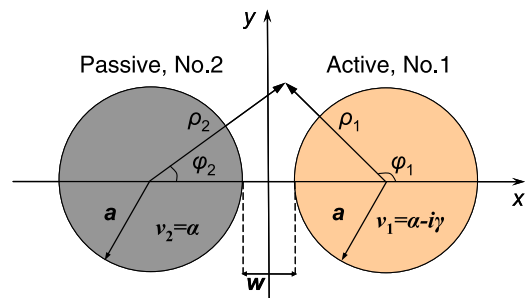


Fig. 1. In-plane geometry of two optically coupled circular disk microresonators, active (right) and passive (left).

where  $J_m$  is the Bessel function, and  $S_p(\varphi_i) = \cos p\varphi_i$  for the  $x$ -even modes and  $\sin p\varphi_i$  for the  $x$ -odd modes. In free space, the field function is a superposition of expansions generated by both resonators

$$U(\rho, \varphi) = \sum_{p=0(1)}^{\infty} B_p^1 H_p^{(1)}(k\rho_1) S_p(\varphi_1) + \sum_{p=0(1)}^{\infty} B_p^2 H_p^{(1)}(k\rho_2) S_p(\varphi_2), \quad (2)$$

where  $H_p^{(1)}$  is the Hankel function of first kind.

Then the substitution of Eqs. (1) and (2) into the boundary conditions, use of the Graf addition theorems, and rescaling of unknown coefficients as  $x_m = A_m^1 F_m(\kappa, \nu_1) J_m(\kappa)$ , and  $y_m = A_m^2 F_m(\kappa, \nu_2) J_m(\kappa)$ , where

$$F_m(\kappa, \nu_j) = J_m(\kappa\nu_j) H_m^{(1)}(\kappa) - \nu_j \beta^{E,H} J'_m(\kappa\nu_j) H_m^{(1)}(\kappa) \quad (3)$$

and  $\beta_j^E = 1$ ,  $\beta_j^H = \nu_j^{-2}$ , leads to the matrix equations

$$x_m^{\pm} + \sum_{p=0(1)}^{\infty} \mu_p y_p^{\pm} K_{mp}(\kappa, \nu_2) [H_{m-p}^{(1)}(\kappa l) \pm (-1)^p H_{m+p}^{(1)}(\kappa l)] = 0, \quad (4)$$

$$y_m^{\pm} + \sum_{p=0(1)}^{\infty} \mu_p x_p^{\pm} K_{mp}(\kappa, \nu_1) [H_{m-p}^{(1)}(\kappa l) \pm (-1)^p H_{m+p}^{(1)}(\kappa l)] = 0, \quad (5)$$

where the upper indices  $+$  and  $-$  correspond to the  $x$ -even and  $x$ -odd mode classes, respectively,  $l = 2 + w/a$  is the normalized distance between the centers of resonators,  $\mu_0 = 1/2$ ,  $\mu_{p>0} = 1$  and

$$K_{mp}(\kappa, \nu_j) = J_m(\kappa) V_p(\kappa, \nu_j) [F_p(\kappa, \nu_j) J_p(\kappa)]^{-1}, \quad (6)$$

$$V_m(\kappa, \nu_j) = J_m(\kappa\nu_j) J'_m(\kappa) - \nu_j \beta_j^{E,H} J'_m(\kappa\nu_j) J_m(\kappa), \quad j=1,2, \quad (7)$$

where the prime denotes differentiation in argument.

In thin disks,  $E_z$ -polarized modes have much smaller effective refractive indices than the  $H_z$ -polarized ones and hence much higher thresholds. Therefore we will further concentrate our analysis on the  $H_z$ -polarized modes.

The search for the LEP eigenvalues is reduced to finding the zeros of determinants of Eqs. (4) and (5) truncated to the order  $N$ . Note that the cylindrical functions in Eqs. (4) and (5) can be calculated to machine precision. As the equations obtained are the Fredholm second kind matrix equations, the accuracy of finding the eigenvalues is controlled by  $N$ , and the convergence to exact eigenvalues is guaranteed if truncation number  $N \rightarrow \infty$ .

As for the twin-disk PM laser (see Figs. 4 and 5 of [4]), to achieve a practical accuracy of 4 or 5 digits one needs

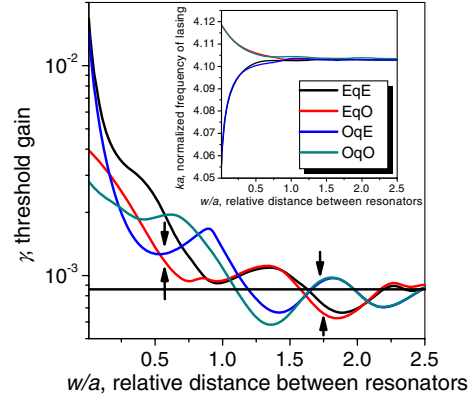


Fig. 2. Threshold values of material gain and the normalized lasing frequencies (inset) for the  $H_z$ -polarized supermodes of the family  $(H_z)_{7,1}$  versus the relative distance,  $w/a$ , between microdisks;  $\alpha = 2.63$  and  $N = 70$ .

a few more equations than the resonator's optical size,  $ka\alpha$ . As an initial guess we took the values for  $\kappa$  and  $\gamma$  in a single active resonator and then used a two-parameter secant-type iterative method [4].

In Fig. 2, we present the dependences of the lasing frequencies and thresholds on the separation parameter,  $w/a$ , four supermodes of two classes built on the  $(H_z)_{7,1}$  modes in each cavity. If the separation  $w$  becomes smaller than  $\sim 0.7a$ , then the modes obtain the same frequency shifts as in a twin-disk PM laser, with their thresholds being twice higher than in the twin-disk laser (not shown here). This behavior is in full agreement with the findings of [14]: if  $w/a < 0.7$ , then the gain-field overlap coefficients are twice smaller than in a twin-disk PM laser studied in [4].

If  $w$  is becoming larger, then both  $\kappa$  and  $\gamma$  tend to the one-disk values (black lines) because the field in the passive disk fades off. In Fig. 3, we present the fading factor,  $F$ , which is the ratio of the maximum value of  $|H_z|$  inside the passive resonator to the maximum value inside the active one. Note that  $F \approx 0.5$  even if  $w \approx a$ .

Near fields of two supermodes of the types  $x$ -odd/ $y$ -quasi-even (OqE) and  $x$ -even/ $y$ -quasi-odd (EqO) are shown in Fig. 4 for a relatively large separation value,  $w/a = 1.75$ , corresponding to the arrows in Figs. 3 and 4.

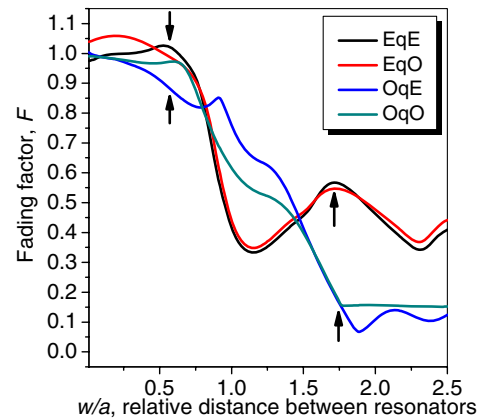


Fig. 3. Fading factors  $F$  for the  $H_z$ -polarized supermodes built on the WG modes  $(H_z)_{7,1}$  versus the relative distance,  $w/a$ , between microdisks;  $\alpha = 2.63$  and  $N = 70$ .

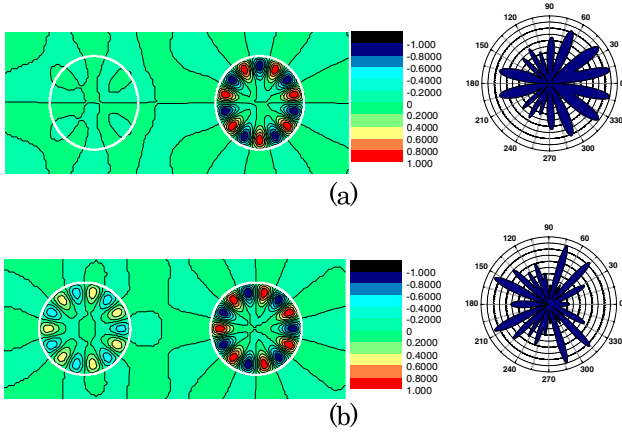


Fig. 4. Near- and far-field patterns  $|H_z|$  for the  $H_z$ -polarized supermodes of the OqE (a) and EqO (b) types, built on the WG modes  $(H_z)_{7,1}$  for widely spaced microdisks,  $w/a = 1.75$ .

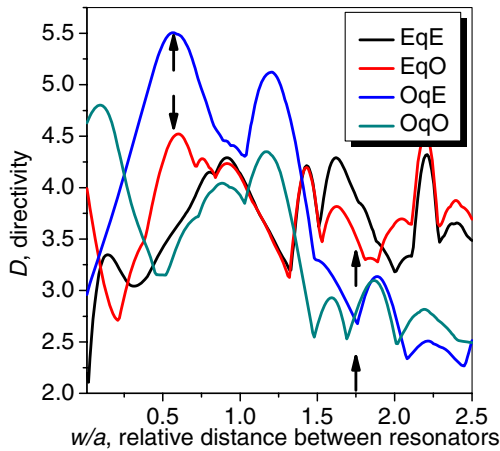


Fig. 5. Directivities for the  $H_z$ -polarized supermodes built on the WG modes  $(H_z)_{7,1}$  versus the relative distance,  $w/a$ , between microdisks;  $\alpha = 2.63$  and  $N = 70$ .

The other important parameter in applications of lasing is the directionality of emission. This quantity can be characterized using the *directivity* borrowed from antenna theory (see [4] for its definition). In Fig. 5, we present the plots of the directivities of the same four supermodes as in Figs. 2 and 3. They show that the directivity of emission can be several times higher than for a single-disk laser value of 2. The maximum values are found for rather closely spaced microcavities, i.e., when both active and passive microcavities shine brightly. The corresponding near and far fields are presented in Fig. 6 and show a noticeably smaller number of comparable beams of emission than those in Fig. 4. Note that the most directive supermode of the  $x$ -even family EqO has one main beam of emission along the line of symmetry and seven smaller intensive sidelobes. All  $x$ -odd modes have a minimum two identical main beams.

The presented results highlight the role of the overlap between the active region and the modal electric field, in the control of the lasing threshold, and have predictive power. Indeed, suppose that we have a cyclic PM of

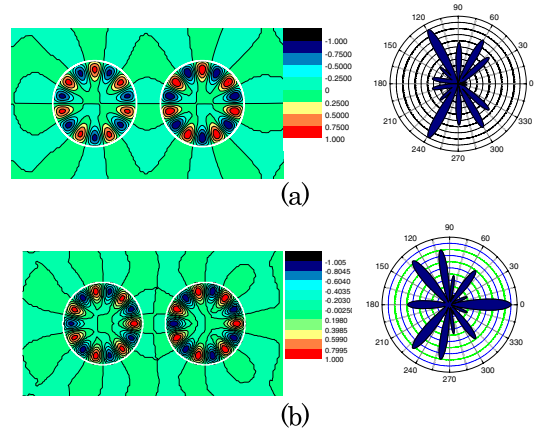


Fig. 6. Near- and far-field patterns  $|H_z|$  for the  $H_z$ -polarized supermodes of the OqE (a) EqO (b) types, built on the WG modes  $(H_z)_{7,1}$  for closely spaced microdisks,  $w/a = 0.57$ .

$M$  identical strongly coupled cavities; however, only  $M_1$  of them are pumped.

Then one can foresee that the mode thresholds will be  $M/M_1$  times higher than for a uniformly pumped PM. This effect can be helpful in the engineering of thresholds of lasing with the aid of selective pumping of individual cavities in PM microlasers [3].

This work was supported, in part, by the National Academy of Sciences of Ukraine via the State Target Program “Nanotechnologies and Nanomaterials.”

## References

1. P. W. Evans and N. Holonyak, Jr., *Appl. Phys. Lett.* **69**, 2391 (1996).
2. S. C. Creagh and M. D. Finn, *J. Phys. A* **34**, 3791 (2001).
3. S. Ishii, A. Nakagawa, and T. Baba, *IEEE J. Sel. Top. Quantum Electron.* **12**, 71 (2006).
4. E. I. Smotrova, A. I. Nosich, T. M. Benson, and P. Sewell, *IEEE J. Sel. Top. Quantum Electron.* **12**, 78 (2006).
5. E. I. Smotrova, A. I. Nosich, T. M. Benson, and P. Sewell, *Opt. Lett.* **31**, 921 (2006).
6. J.-W. Ryu, S.-Y. Lee, C.-M. Kim, and Y.-J. Park, *Phys. Rev. A* **74**, 013804 (2006).
7. S. V. Boriskina, *Opt. Lett.* **32**, 1557 (2007).
8. S. Preu, H. G. L. Schwefel, S. Malzer, G. H. Dohler, L. J. Wang, M. Hanson, J. D. Zimmerman, and A. C. Gossard, *Opt. Express* **16**, 7336 (2008).
9. X. Li, R. C. Myers, F. M. Mendoza, D. D. Awschalom, and N. Samarth, *IEEE J. Quantum Electron.* **45**, 932 (2009).
10. C. Schmidt, A. Chipouline, T. Käsebier, E.-B. Kley, A. Tünnermann, T. Pertsch, V. Shuvayev, and L. I. Deych, *Phys. Rev. A* **80**, 043841 (2009).
11. M. Benyoucef, J.-B. Shim, J. Wiersig, and O. G. Schmidt, *Opt. Lett.* **36**, 1317 (2011).
12. C. Schmidt, M. Liebsch, A. Klein, N. Janunts, A. Chipouline, T. Kasebier, C. Etrich, F. Lederer, E.-B. Kley, A. Tünnermann, and T. Pertsch, *Phys. Rev. A* **85**, 033827 (2012).
13. A. I. Nosich, E. I. Smotrova, S. V. Boriskina, T. M. Benson, and P. Sewell, *Opt. Quantum Electron.* **39**, 1253 (2007).
14. E. I. Smotrova, V. O. Byelobrov, T. M. Benson, J. Ctyroky, R. Sauleau, and A. I. Nosich, *IEEE J. Quantum Electron.* **47**, 20 (2011).